NeuroImage 200 (2019) 332–343

Contents lists available at ScienceDirect

NeuroImage

journal homepage: www.elsevier.com/locate/neuroimage

Visual imagery during real-time fMRI neurofeedback from occipital and superior parietal cortex

Patrik Andersson [a,b,*,1], Flavio Ragni [a], Angelika Lingnau [a,c,d]

[a] Center for Mind/Brain Sciences (CIMeC), University of Trento, 38068, Italy
[b] Stockholm University Brain Imaging Centre, Stockholm University, 106 91, Stockholm, Sweden
[c] Department of Psychology, Royal Holloway University of London, TW20 0EX, UK
[d] Institute of Psychology, University of Regensburg, 93053, Regensburg, Germany

ARTICLE INFO

Keywords:
Visual imagery
Real-time fMRI
Visual network
Medial superior parietal lobe
Self-regulation

ABSTRACT

Visual imagery has been suggested to recruit occipital cortex via feedback projections from fronto-parietal regions, suggesting that these feedback projections might be exploited to boost recruitment of occipital cortex by means of real-time neurofeedback. To test this prediction, we instructed a group of healthy participants to perform peripheral visual imagery while they received real-time auditory feedback based on the BOLD signal from either early visual cortex or the medial superior parietal lobe. We examined the amplitude and temporal aspects of the BOLD response in the two regions. Moreover, we compared the impact of self-rated mental focus and vividness of visual imagery on the BOLD responses in these two areas. We found that both early visual cortex and the medial superior parietal cortex are susceptible to auditory neurofeedback within a single feedback session per region. However, the signal in parietal cortex was sustained for a longer time compared to the signal in occipital cortex. Moreover, the BOLD signal in the medial superior parietal lobe was more affected by focus and vividness of the visual imagery than early visual cortex. Our results thus demonstrate that (a) participants can learn to self-regulate the BOLD signal in early visual and parietal cortex within a single session, (b) that different nodes in the visual imagery network respond differently to neurofeedback, and that (c) responses in parietal, but not in occipital cortex are susceptible to self-rated vividness of mental imagery. Together, these results suggest that medial superior parietal cortex might be a suitable candidate to provide real-time feedback to patients suffering from visual field defects.

1. Introduction

Visual imagery refers to the representation and experience of a visual image in the absence of external visual stimulation. Earlier studies on visual imagery relied on behavioral paradigms and subjective measures (for reviews, see e.g. Kosslyn et al. (2001) and Pearson et al. (2015)). More recently, using functional neuroimaging, visual imagery has been shown to activate a vast network of brain areas, including the visual cortex, but also parietal, temporal and frontal regions (de Borst et al., 2012; Gourtzelidis et al., 2005; Hamamé et al., 2012; Whittingstall et al., 2014; Zvyagintsev et al., 2013). Early visual cortex has been shown to be recruited in the same retinotopically organized way during visual imagery as during perception (Klein et al., 2004; Slotnick et al., 2005; Wandell et al., 2007), indicating that imagery and perception have similarities in the processing of low-level visual features (Albers et al., 2013; Emmerling et al., 2016; Lee et al., 2012). However, whereas early visual cortex is recruited in a bottom-up, stimulus-driven manner during perception, it is assumed that during visual imagery, in the absence of visual stimulation, early visual cortex is recruited via top-down signals from fronto-parietal areas (Dentico et al., 2014; Dijkstra et al., 2017b; Mechelli et al., 2004).

These observations raise the intriguing question whether visual imagery could be used for rehabilitation of visual impairments such as neglect (Robineau et al., 2017; Smania et al., 1997) and partial visual field loss (scotoma) after stroke (Papageorgiou et al., 2014). While compensatory eye-movement strategies (Trauzettel-Klosinski, 2011; Urbanski et al., 2014) have traditionally been used for patients suffering from visual field loss, there is now a growing interest in restorative

* Corresponding author. Center for Mind/Brain Sciences (CIMeC), University of Trento, Corso Bettini 31, 38068, Rovereto, Italy.
E-mail address: patrik.andersson@su.se (P. Andersson).
[1] Present address: Stockholm University Brain Imaging Centre (SUBIC), Department of Linguistics, 106 91 Stockholm, Sweden.

https://doi.org/10.1016/j.neuroimage.2019.06.057
Received 8 December 2018; Received in revised form 11 June 2019; Accepted 24 June 2019
Available online 25 June 2019

training (Matteo et al., 2016; Urbanski et al., 2014). In contrast to compensatory strategies, the idea of restorative training is to restore part of the visual field by utilizing the ability of the visual network to perform plastic changes and structurally and functionally adapt to the damage. While it has been shown that the visual system can plastically reorganize (Brodtmann et al., 2015; Hübener and Bonhoeffer, 2014), it is not currently known to what extent and how to best help this reorganization to take place. A better understanding of how to exploit the brain's capacity for plastic recovery will be an important part of designing restorative rehabilitation strategies. In some patients, repetitive (bottom-up) visual stimulation has been suggested to be able to induce rehabilitory plastic changes at the visual field border of, or in islands of residual vision within, a scotoma (Dundon et al., 2015; Sabel et al., 2011; Urbanski et al., 2014). The underlying idea is that reactivating the cells in partially damaged regions leads to strengthening of synaptic transmission and synchronization of structures and networks (Sabel et al., 2011). A suggested alternative, or supplementary, strategy is to instead reactivate the damaged regions via top-down imagery processes (Papageorgiou et al., 2014).

One of the problems related to the use of visual imagery in rehabilitation is the fact that there exist considerable individual differences in the strength of imagery induced activation, in particular in early visual cortex (Klein et al., 2004; Kosslyn and Thompson, 2003; Slotnick et al., 2005). Moreover, when studying completely covert mental processes, such as visual imagery, participants can often be uncertain on their ability to perform the task. By providing real time feedback of the BOLD signal from relevant cortical regions, participants can learn to use the feedback to improve the ability to self-regulate these regions, thereby potentially boosting an otherwise weak signal. Real-time fMRI (RT-fMRI) (Cox et al., 1995; Sulzer et al., 2013) neurofeedback has been proven to facilitate self-regulation of a variety of regions, including visual areas (Andersson et al., 2011; Scharnowski et al., 2012). Scharnowski et al. (2012, 2014) demonstrated that participants trained in up-regulating early visual cortex had an enhanced perceptual sensitivity in the part of the visual field corresponding to the trained region.

In stroke patients, the partially damaged cortical region that is the target for restorative training can be expected to have a compromised BOLD signal due to the small number of functioning cells and an impaired cerebrovascular reactivity (de Haan et al., 2013; Pleger et al., 2003). Thus, in order to get a useable feedback signal, the target region for the neurofeedback could potentially better be a region in an undamaged node of the top-down visual network recruited during visual imagery. Given its role in top-down projections to occipital cortex during visual imagery (Dentico et al., 2014; Mechelli et al., 2004), parietal cortex might thus be a suitable candidate target region. It is however not clear how a higher level region will behave during neurofeedback learning, and how this behavior transfers to early visual cortex.

In this study we hypothesized that it is possible to learn self-regulation of the BOLD signal in MSPL using RT-fMRI neurofeedback during peripheral visual imagery. We therefore examined the effect of visual imagery during RT-fMRI neurofeedback targeting both the low level visual cortex (V1–V3) and the medial superior parietal lobe (MSPL) in a group of normal-sighted participants. MSPL is involved in processing spatial visual information and is thought to be a hub that connects several nodes in the visual network (Gourtzelidis et al., 2005; Pflugshaupt et al., 2016). The region has also been shown to be recruited during visual imagery (de Gelder et al., 2015; Filimon et al., 2007; Trojano et al., 2002), but not to be sensitive to content of the imagined images (Mechelli et al., 2004). Based on these properties, MSPL might be a good candidate region to provide feedback for visual imagery targeting a specific spatial location, as it is the case in patients with visual field defects.

Based on the different roles of early visual cortex and parietal cortex in the visual processing network, we aimed to compare their behavior and characteristics during visual imagery. Moreover, given the known individual differences in the strength of imagery induced activation (Klein et al., 2004; Kosslyn and Thompson, 2003; Slotnick et al., 2005), we were interested in possible differences between these two regions in how mental focus and vividness of visual imagery impact their responses, an effect that to date has mainly been studied in early visual cortex (Cui et al., 2007; Pearson et al., 2015). To do so, we provided participants with auditory real-time feedback either from early visual cortex or from MSPL in two separate sessions while they performed visual imagery. We hypothesized that the BOLD signal in both target regions is affected by the participant's instantaneous mental capacity to focus on the task. To compare the impact of mental focus and vividness of visual imagery on the BOLD response in early visual and parietal cortex, participants provided ratings of their mental focus and the vividness of visual imagery for each individual run at the end of each session. Moreover, the analysis of the impact of the up- and down-regulation on other regions that are part of the same functional network, but that were not targets of the feedback, can potentially provide additional insights into their roles in the network.

2. Material and methods

2.1. Experimental design

All participants completed two scanning sessions with 6–7 days apart (see Fig. 1). For the experimental group (N = 14), one of the real-time feedback sessions targeted a region located in the occipital lobe while the other session targeted the MSPL. Half of the participants were randomly selected to start with feedback from the occipital target region. Participants in the control group (N = 7) unknowingly received feedback from bilateral ventral striatum in both sessions, a region not previously reported to be recruited during visual imagery. Besides unknowingly having a different target for the feedback, the control participants were provided with exactly the same instructions and information as the participants from the experimental group. Before the participant was placed inside the scanner we explained that the effect that we base the feedback on (hemodynamic response) has a delay of several seconds before it appears and that it takes time before it disappears. We also stressed the importance of keeping the gaze focused on the central fixation cross at all times and keeping the head still.

The target regions were defined using two functional localizer runs that initiated each session (Fig. 1; for details, see section Localizers). The first run of each session was a stimulus localizer (Fig. 2A), containing alternating blocks of upper left and upper right visual stimulation, and was used to define a Region of Interest (ROI) in early visual cortex (ROI_O). The second run was an imagery localizer (Fig. 2B) and instead contained blocks of upper left and upper right visual imagery of the same stimuli displayed in the stimulus localizer. These data were used to define an ROI in the MSPL (ROI_P). The two localizers were followed by two runs with real-time feedback from either ROI_O or ROI_P (Fig. 2C). During

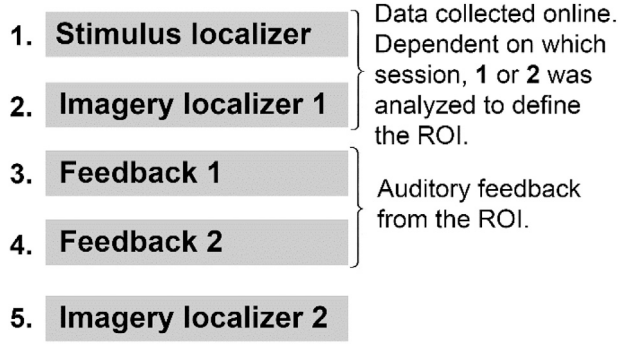

Fig. 1. Overview of a single session. Each participant attended two separate scanning sessions. For the experimental group, one session targeted an occipital ROI (from Stimulation localizer) and the other session targeted a parietal ROI (from Imagery localizer 1). Participants in the control group received feedback from the ventral striatum in both sessions.

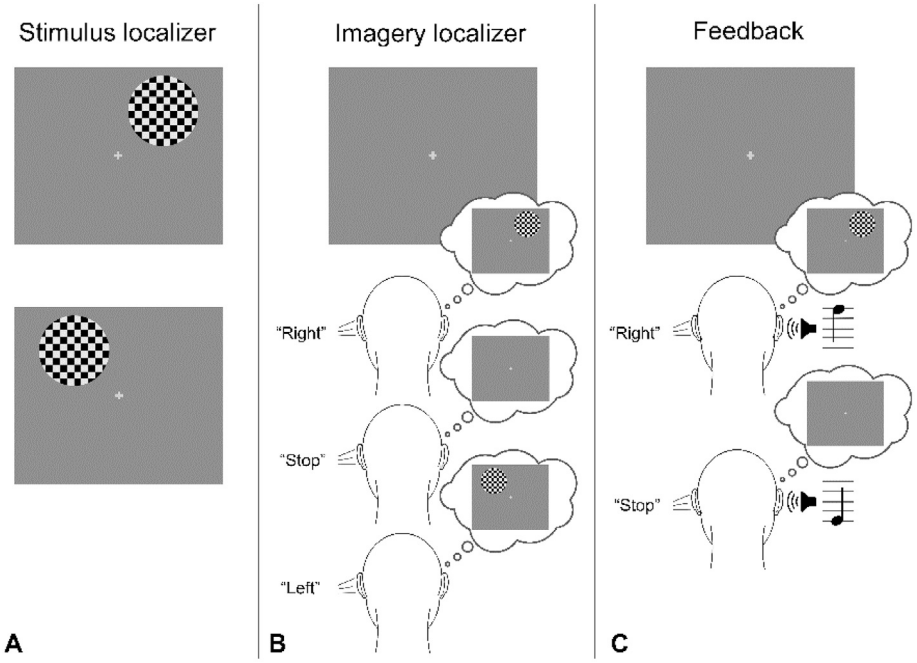

Fig. 2. During all three tasks the participants fixated their gaze on a central fixation cross. (A) The stimulus localizer consisted of a flickering checkerboard pattern presented in the upper right or left visual field. (B) During the imagery localizer participants were verbally instructed to imagine the flickering circle in one of the two quadrants, or to stop imagining during rest blocks. (C) Real-time feedback runs contained blocks of upper right imagery and rest blocks. The feedback, representing the activity in the ROI, was communicated via the frequency of a beep sound played at every TR.

feedback runs participants were instructed to perform visual imagery in the upper right quadrant (for details, see section '2.6 Real-time feedback'). After the two feedback runs we collected one more run with the imagery localizer which served as comparison to the pre-feedback imagery localizer. Due to participants' fatigue over time, the second imagery localizer also increased the chances of collecting data with a larger spread in ratings of vividness and focus and that could be used for investigating their effect on the BOLD signal.

2.2. Participants

Twenty-one healthy volunteers participated in the study. Seven of the participants were randomly selected to be in the control group (experimental group: N = 14, 7 females, age min/max/mean 19/31/23.6; control group: N = 7, 4 females, age min/max/mean 19/30/24.7). All participants had normal or corrected-to-normal vision and had no history of neurological or psychiatric disease. Before starting the experiment, all participants gave written informed consent. The study was approved by the Ethics Committee for research involving human subjects at the University of Trento, Italy.

2.3. MR data

Data were collected using a 4T Bruker MedSpec Biospin MR scanner equipped with an eight-channel birdcage head coil. T1-weighted structural images were acquired using an MPRAGE sequence (TI/TR/TE = 1020/4.18/2700 m s, FA = 7°, FOV = 256 × 224 mm, 176 slices, 1 mm isotropic resolution, GRAPPA acceleration factor = 2). Functional data were acquired using an EPI sequence (TR/TE = 2000/30 m s, flip angle = 73°, matrix size = 64 × 64, 29 interleaved slices, slice thickness = 3.6 mm, in-slice resolution 3 mm). Slices were axial, slightly oblique to optimize brain coverage.

2.4. Subjective rating data

Directly after being taken out of the scanner, participants were asked to fill in a questionnaire where they rated their mental focus and imagery vividness, separately for each imagery localizer and feedback run. These values allowed us to correlate changes in the peaks of the BOLD response in all runs to changes in self-rated focus and vividness using the Spearman's rank correlation coefficient. It also allowed us to do a separate analysis on runs rated by the participants as high focus. This would not have been possible with the standard Vividness of Visual Imagery Questionnaire (VVIQ) (Marks, 1973) that would only give us a general level of vividness for each participant and no rating of their focus. However, we kept the scale (1–5) applied in the VVIQ for ease of comparison. The answer alternatives for rating vividness were: 1. *Perfectly clear and as vivid as normal vision*; 2. *Clear and reasonably vivid*; 3. *Moderately clear and vivid*; 4. *Vague and dim*; 5. *No image at all (only "knowing" that I was thinking of the object)*. The answer alternatives for rating focus were: 1. *I was completely focused on the task the whole time*; 2. *I was focused on the task most of the time*; 3. *I was sometimes focused on the task, but sometimes not*; 4. *I had trouble focusing on the task most of the time*; 5. *I never managed to focus on the task.*

2.5. Localizers

Both localizers were implemented in ASF (Schwarzbach, 2011), a toolbox based on the Psychophysics Toolbox (Version 3) (Brainard, 1997), using MATLAB 8.3 (Mathworks, Natick, USA). The same MATLAB version was used for data analysis.

During the stimulus localizer, participants were presented with a circular flickering (10 Hz) checkerboard pattern presented either in the upper right or upper left quadrant (Fig. 2A). There were 8 blocks of 10 s for each location, without separation. The circle was located 3.5° from the centre and had a radius of 1.9° visual angle. Participants were instructed to fixate a central cross at all times.

During the imagery localizer the screen only contained the fixation cross and the instructions were delivered verbally via headphones (Fig. 2B). The instructions were recordings of the words "Right" and "Left" for visual imagery in the upper right and left visual field, respectively. The imagery localizer consisted of eight alternating 16 s blocks of visual imagery in the right and left visual field, where each imagery block was followed by an equally long rest block (instructed by the word "Stop"). The blocks were longer in the imagery localizer compared to in the stimulus localizer to compensate for the fact that the covertly imagined image takes some time to build up.

Data were collected on-the-fly during the localizers and, once

finished, the relevant dataset was analyzed with a standard general linear model (GLM) using SPM8 (http://www.fil.ion.ucl.ac.uk/spm/software/spm8/). If a participant was scheduled to receive feedback from the occipital cortex, the stimulus localizer was analyzed to identify ROI_O. By contrast, if the participant was scheduled to receive feedback from parietal cortex, the imagery localizer was used to identify ROI_P. We applied the contrast "right-left" for both the stimulus and imagery localizers to locate brain regions recruited during perception and visual imagery, respectively, in the upper right quadrant. Using this contrast for ROI selection, we avoided including regions responding more generally, and not retinotopically, to the localizer tasks. Note that the responses during visual imagery in the left visual field are never included in any of the averages or plots in the Results (except for Fig. 10, where it is explicitly stated). ROI_O, from the stimulus localizer, was defined as the 50 voxels with the highest t-values in the left occipital lobe; clusters smaller than 3 voxels were removed. When defining ROI_P from the imagery localizer, we used a combination of anatomical and functional criteria. First, we located the left superior precuneus in the middle sagittal slice, moved 5 slices (15 mm) into the left hemisphere and from there defined a sphere with a radius of 15 mm. Inside this sphere we selected the 20 voxels with the highest t-values with clusters smaller than 3 voxels removed. The decision to use this number of voxels was based on previous pilot experiments that showed it to be a reasonable size considering the large inter-subject variability in activation.

Due to a technical malfunction, the data from the imagery localizer for one of the participants was not saved. However, this was in the session targeting the occipital region where the target ROI is defined using the stimulus localizer.

The bilateral ventral striatum ROI, that served as feedback target for the control group, was manually selected using one of the functional EPI images (see also Fig. 8).

2.6. Real-time feedback

During feedback runs (Fig. 2C), participants were instructed to imagine the same flickering checkerboard pattern as before, but were allowed to visualize another image to potentially improve their performance, as long as it was localized to the same region of their visual field and not static. Table 1 provides details on the images participants reported to use.

Every feedback run started with 30 s of rest from which the mean and standard deviation of the BOLD signal in the ROI voxels were estimated and used for normalizing the amplitude of each voxel's time series. The maximum average inside the ROI during the 30 s, S_{max}, was also computed and used for scaling the feedback. The initial rest period was followed by nine 24 s blocks of upper right imagery separated by equally long rest blocks. The average normalized signal inside the ROI was transformed to an auditory frequency where the interval $[-3 \times S_{max}, 3 \times S_{max}]$ was mapped to the auditory frequency interval [200 Hz, 1000 Hz] via 21 evenly spaced levels. The auditory tone represented only the last sample of brain activity since no averaging was performed on the data over time. Participants were instructed to try to achieve a high frequency sound during imagery blocks and a low frequency sound during rest. By using auditory feedback we minimized the risk of

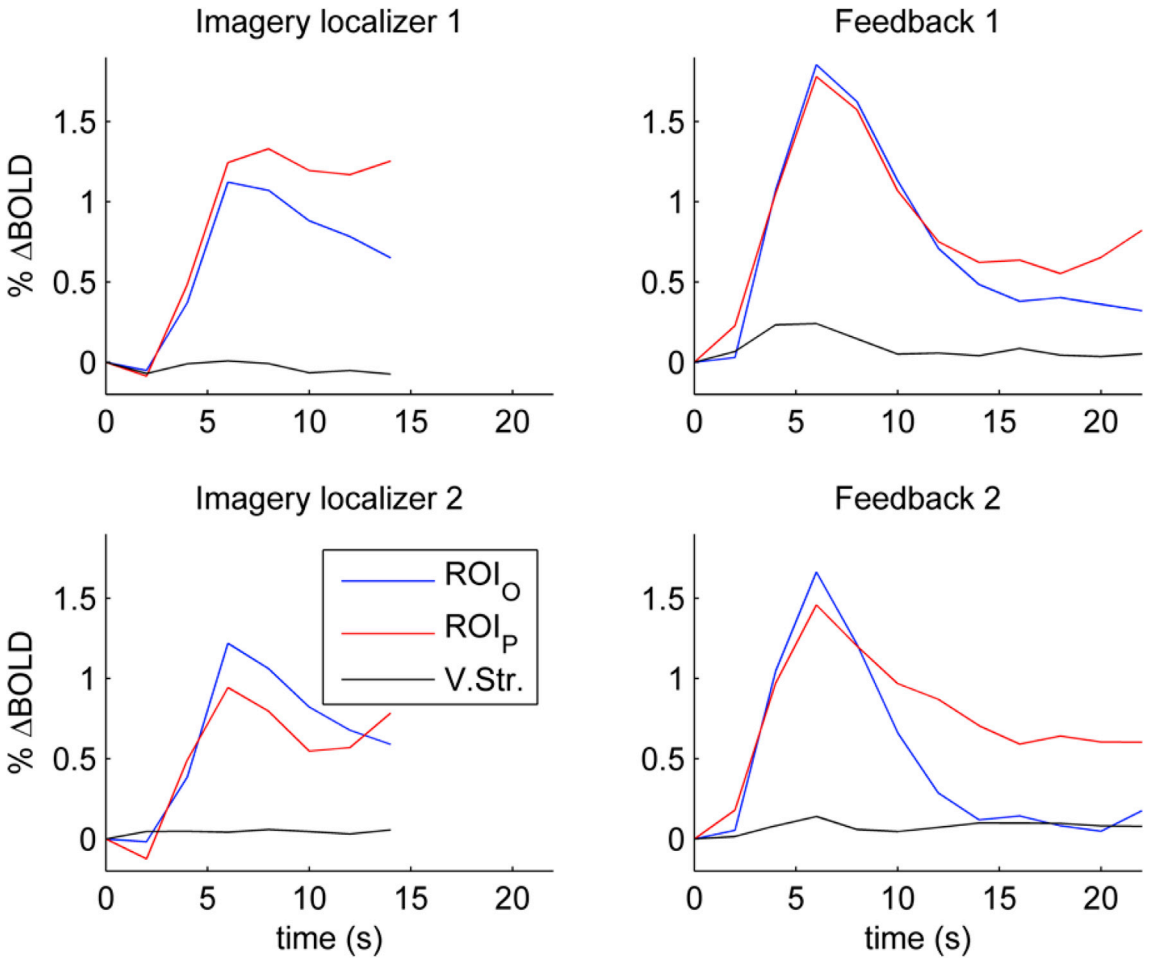

Fig. 3. The average BOLD responses for the experimental group in ROI_O (blue) and ROI_P (red) during the two imagery localizers (left column) and the two feedback runs (right column). The order of the runs within the session is: Imagery localizer 1, Feedback 1, Feedback 2, Imagery localizer 2. The black curve shows the average responses for the control group inside bilateral ventral striatum (V.Str.).

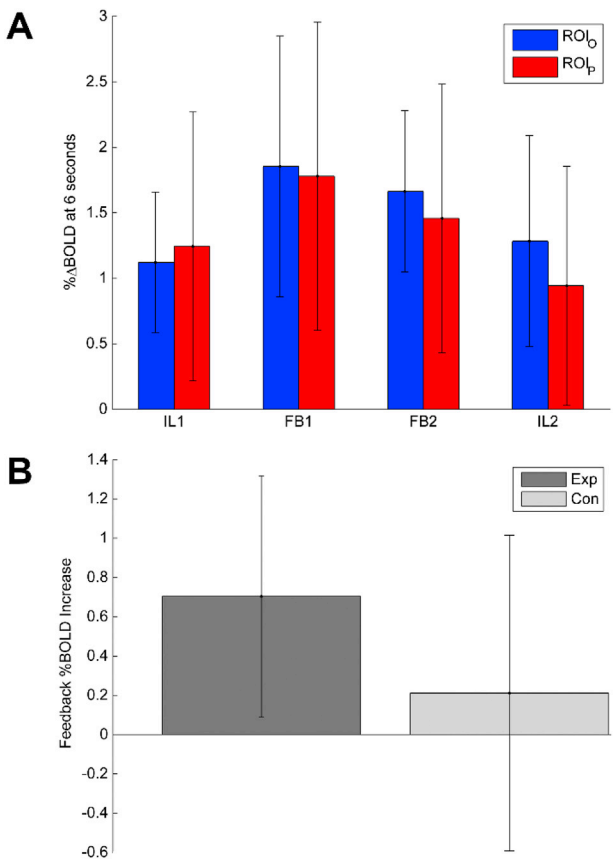

Fig. 4. (A) The mean response amplitude at the 6s peak inside ROI_O and ROI_P for the different functional runs. (B) Mean increase in response amplitude from imagery localizer 1 to (collapsed) feedback run 1 and 2 at the 6s peak inside ROI_O. Dark and light gray bars represent the experimental (Exp) and control (Con) groups, respectively. Note that ROI_O for control participants was computed offline for comparison purposes, while feedback was given from bilateral ventral striatum. Error bars represent the standard deviation.

unwanted interference with visual processing.

Functional image volumes were exported to a directory in Analyze format directly following reconstruction. The RT-fMRI software, implemented in MATLAB and run on a laptop (HP ZBook 15G2, 16 GB RAM, Intel Core i7-4710MQ 2.50 GHz processor) with Windows 7 operating system, picked up new data as available and processed it to update the feedback. Image volumes were rigidly coregistered to the first volume of the localizer run used for creating the ROI, and a high-pass filter (cut-off 0.029 Hz) was applied on each voxel's time signal.

After an image volume had been scanned, it took on average 200 m s before it was available to read from disk and then 390 m s of data processing before feedback was sent.

2.7. Whole brain analysis

In order to identify areas recruited during visual imagery at the group level, we normalized all participants' data to the Montreal Neurological Institute (MNI) template space using SPM8. T1 images were segmented into different tissue types using the 'New Segment' option. Using DARTEL (Ashburner, 2007), participants' anatomical scans were first iteratively aligned to a mean template and subsequently fitted to the MNI template. The estimated deformations were then applied to all the imagery localizer and feedback data, reinterpolated to 3 mm isotropic resolution and smoothed with a 6 mm Gaussian kernel, as well as all ROIs, also reinterpolated to 3 mm isotropic resolution but not smoothed.

Next, we performed an offline random-effects (RFX) group analysis on the data of imagery localizer 1 (from both sessions). Group-level statistical maps were computed using one-sample t-tests on the contrast images ("imagery right - imagery left" and "imagery right + imagery left") from the first-level GLM analysis on the subject level. Whereas the contrast "imagery right – imagery left" served to identify voxels that showed spatial selectivity during visual imagery, we used the contrast "imagery right + imagery left" to identify clusters more generally recruited during visual imagery, towards both hemifields.

3. Results

3.1. ROI analysis

The size and number of clusters for ROI_O and ROI_P, together with the peak t values, are shown in Table 2. Not surprisingly, the statistics from visual stimulation is much higher than from visual imagery. Table 1 lists the self-reported types of images imagined by the participants during feedback runs, where they were allowed to use alternatives to the checkerboard.

To compare the BOLD responses in ROI_O, ROI_P and the control ROI (bilateral ventral striatum) during visual imagery, we computed the average response across all participants and trials, separately for the two imagery localizers (one before, one after the feedback runs) and the two feedback runs. Percent signal change was calculated in reference to the end (2 TRs) of the preceding rest block. As can be seen in Fig. 3, the signal peaked in both the occipital ROI (blue) and the parietal ROI (red) at around 6 s after instructions. Fig. 3 also suggests that the activation in the parietal ROI might be sustained longer after the peak than in the occipital ROI. As expected, for control participants, visual imagery did not have a significant effect on the BOLD signal in their target region (ventral striatum, black).

As shown in Fig. 4A, the signal peaks are higher in the feedback runs than in the imagery localizers, indicating that participants profited from the real-time feedback to up-regulate the BOLD signal. We tested this observation statistically by comparing the experimental group and the control group in what effect feedback had on the occipital activation. To do this, we first computed an ROI_O for each control participant in the same way as was done for the experimental group during the experiment. We then computed the average amplitude inside ROI_O at the 6 s peak, both in the imagery localizer 1 and in the (collapsed and combined) feedback runs 1 and 2. Finally, we used these values to compute the amplitude increase from the pre-feedback imagery localizer 1 to when they received feedback. Fig. 4B shows the average increase for the control group and the experimental group. The experimental group showed a significantly higher increase compared to the control group (two-sample t-test, $p = 0.044$, $mean_{Exp} \pm SD_{Exp} = 0.70 \pm 0.61$, $mean_{Con} \pm SD_{Con} = 0.21 \pm 0.80$). The effect is modest, but we know from previous studies (Scharnowski et al., 2012; Stoeckel et al., 2014) that the effect of neurofeedback training increases over time. Since our values came from the participants' first or second session, we did not expect a large effect.

Both Figs. 3 and 4A show that the ability to up-regulate the BOLD signal tended to decrease over time in the session. The focus ratings in the questionnaires, as well as verbal communication with the participants, revealed that many of them got tired towards the end of the session.

We computed the BOLD signal in the parietal and the occipital ROIs at the 6 s peaks in both of the imagery localizers and both feedback runs for each participant in the experimental group and compared these values to the rated vividness and focus. Note that, in contrast to the other analyses, data were collapsed across imagery localizers and feedback runs for Fig. 5 and Table 3 since for this analysis we were only interested in the effect of vividness and focus, not in comparing between localizers and feedback. Fig. 5 shows the averaged BOLD peak values sorted according to the ratings of focus and vividness. Both vividness and focus clearly have a considerably stronger effect on the signal in the parietal ROI (Fig. 5, lower panel) than in the occipital ROI (Fig. 5, upper panel). We also computed the Spearman's rank correlation coefficient between the

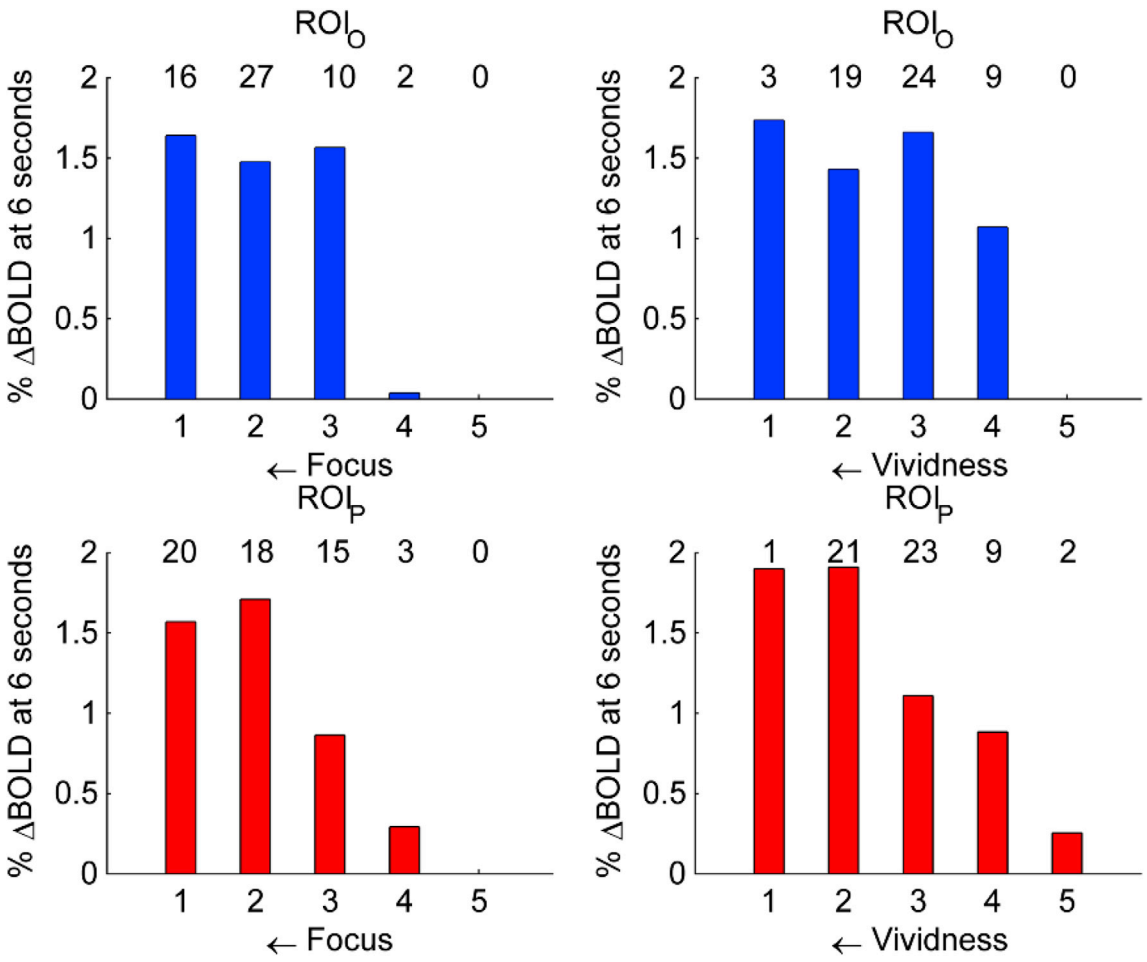

Fig. 5. The mean response at the 6s peak inside ROI_O (upper) and ROI_P (lower) for all imagery localizers and feedback runs, ordered according to the subjectively rated focus and vividness. The numbers above the bars show the number of runs for which this rating was given.

subjective ratings and the BOLD signal peaks. The four correlation values, together with the p-values (for testing the hypothesis of no correlation), can be seen in Table 3. The parietal ROI was significantly correlated to both vividness and focus while the occipital ROI did not show any significant correlation.

When averaging the responses only for runs rated as focus<3 (high focus) the ROI_P curves show an even higher tail compared to the ROI_O curves (Fig. 6) than in Fig. 3. The average amplitude in feedback run 1 and 2 for t > 6s (to the end of the block at 24 s) was significantly higher in ROI_P than in ROI_O (two-sample *t*-test, $p = 0.010$, $mean_O \pm SD_O = 0.51 \pm 0.82$, $mean_P \pm SD_P = 1.16 \pm 0.97$).

We further investigated whether the more sustained activations in ROI_P were also manifested in the occipital region during feedback, even though this region was not the target. To this end, we defined an ROI_O from the stimulus localizer in the ROI_P-feedback session offline and compared the response to when the feedback was targeting ROI_O. The extracted data was processed in the same way as online and the average signal for t > 6s was computed. However, the results showed no significant difference in amplitude. This suggests that feedback from the more sustained parietal region did not help in learning to prolong occipital activity. However, considering that our result is based only on a single training session of ROI_P feedback, this needs to be investigated further.

3.2. Whole brain analysis

The results from the group level *t*-test "imagery right – imagery left" in the imagery localizer 1 data revealed two clusters in the left occipital lobe (Fig. 7) ($p < 0.05$, FWE corrected, cluster extent > 10 voxels).

The cluster dorsal to the calcarine sulcus was not expected considering the upper visual field is processed in the ventral parts of V1–V3. The two most likely explanations are that either this activation represents V3A or V3B, or the imagined image frequently crossed the horizontal meridian. Note that the group analysis did not reveal any significant activation in the MSPL, the region we identified using this localizer. This was however anticipated since our pilot experiments had shown a substantial inter-subject variability in amount and location of the activation pattern. However, the fact that participants were able to up- and down-regulate ROI_P shows that the area is indeed involved in visual imagery.

Fig. 8 displays group maps of all the participants' ROIs after they have been transformed to MNI space. Note that the transformation involves smoothing which e.g. makes the ROI_P map cross the parieto-occipital sulcus even though all ROIs were parietal in subject space.

The group statistics of the contrast "imagery right + imagery left" in the imagery localizer 1 data identified 8 significant clusters involved more generally during visual imagery, towards both hemifields (Fig. 9 and Table 4). The regions were: (left and right) supplementary motor area (SMA), left anterior insula (L-AI), left and right frontal eye fields (FEF), left and right intraparietal sulci (IPS) and left and right premotor cortex (PMC).

Fig. 10 displays the responses inside these 8 clusters during visual imagery in both the left and the right hemifields.

Similar to Fig. 5 and Table 3, we sorted the average 6 s peak values (during visual imagery in the right visual field) for these clusters in the imagery localizers and feedback runs according to their vividness and focus ratings (Fig. 11) and computed the Spearman's rank correlation coefficients (Table 5). For both focus and vividness, the biggest effect was

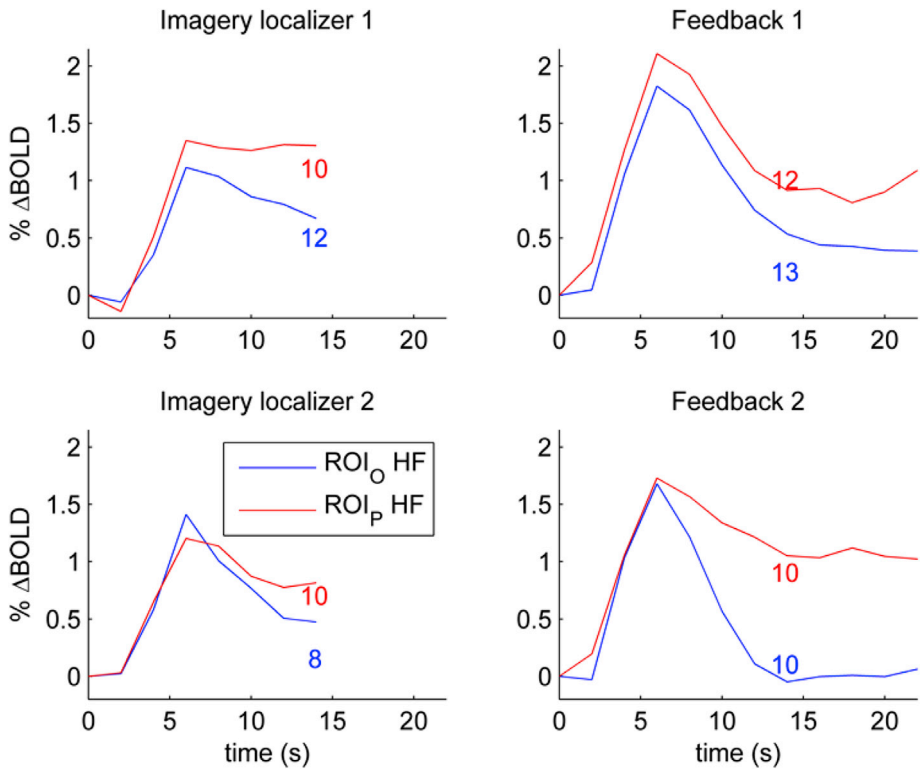

Fig. 6. The average BOLD responses for the experimental group in the runs rated as "high focus" (HF, focus<3). The numbers next to the lines indicate the number of participants included in the average.

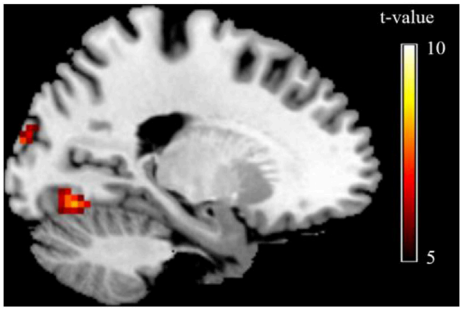

Fig. 7. Regions revealed by the RFX group analysis of imagery localizer 1 for the contrast "imagery right - imagery left", the same contrast used for creating ROI$_P$ ($p < 0.05$, FWE corrected, cluster extent > 10 voxels).

found in L-IPS. The only areas not showing a significant effect ($\alpha = 0.01$) were SMA for both focus and vividness, and R-PMC for vividness.

4. Discussion

Real-time feedback is known to facilitate learning self-regulation with benefits increasing over time (Scharnowski et al., 2012; Stoeckel et al., 2014). Our results show that participants can control brain activity both in early visual cortex and the medial superior parietal lobe by means of visual imagery, and that such effects can be shown within only one feedback session per target region. Moreover, we observed that early visual cortex and the MSPL respond differently, with the BOLD signal in the medial superior parietal lobe being more affected by focus and vividness of visual imagery than early visual cortex. In the following, we will discuss these results in more detail.

4.1. The effect of focus and vividness

A current theory is that parietal cortex provides top-down signals to occipital cortex (Dentico et al., 2014; Mechelli et al., 2004), and that early visual cortex serves as an active 'blackboard' where features can be

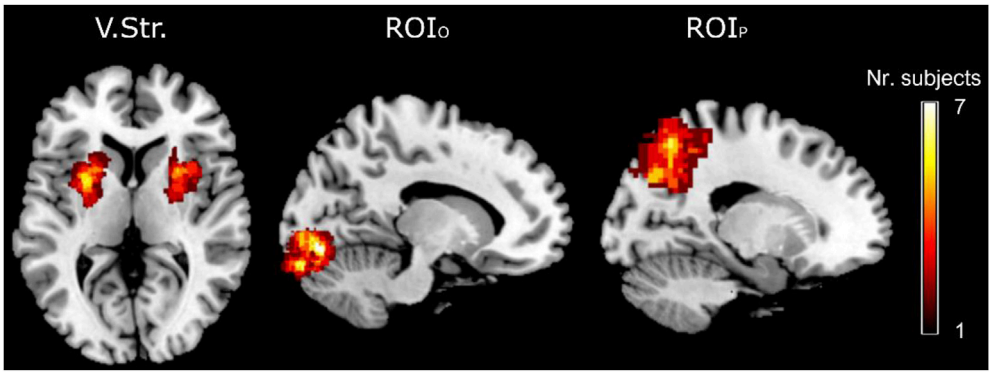

Fig. 8. Group maps of the three types of ROI transformed to MNI space. The scale represents how many subjects had a location covered by a particular ROI.

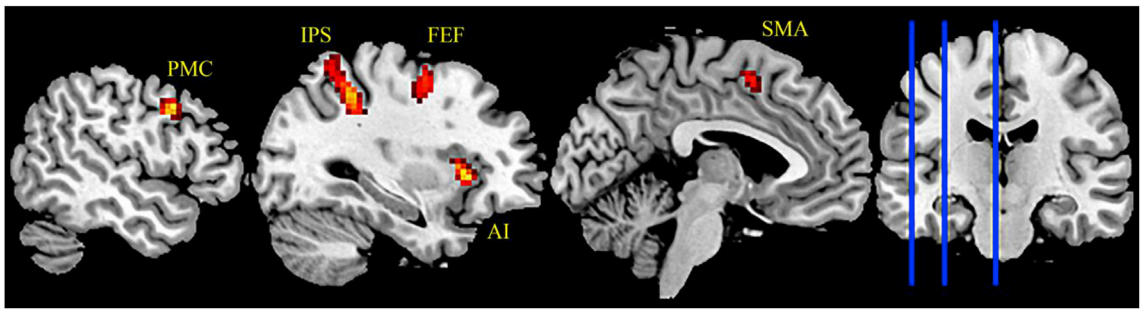

Fig. 9. Significant regions detected by the group analysis of imagery localizer 1 for the contrast "imagery right + imagery left" ($p < 0.05$, FWE corrected, cluster extent > 10 voxels): Supplementary motor area (SMA), left anterior insula (AI), left and right frontal eye fields (FEF), left and right intraparietal sulci (IPS) and left and right premotor cortex (PMC). The figure only presents the regions in the left hemisphere; MNI coordinates of all regions can be found in Table 4. Scale same as in Fig. 7.

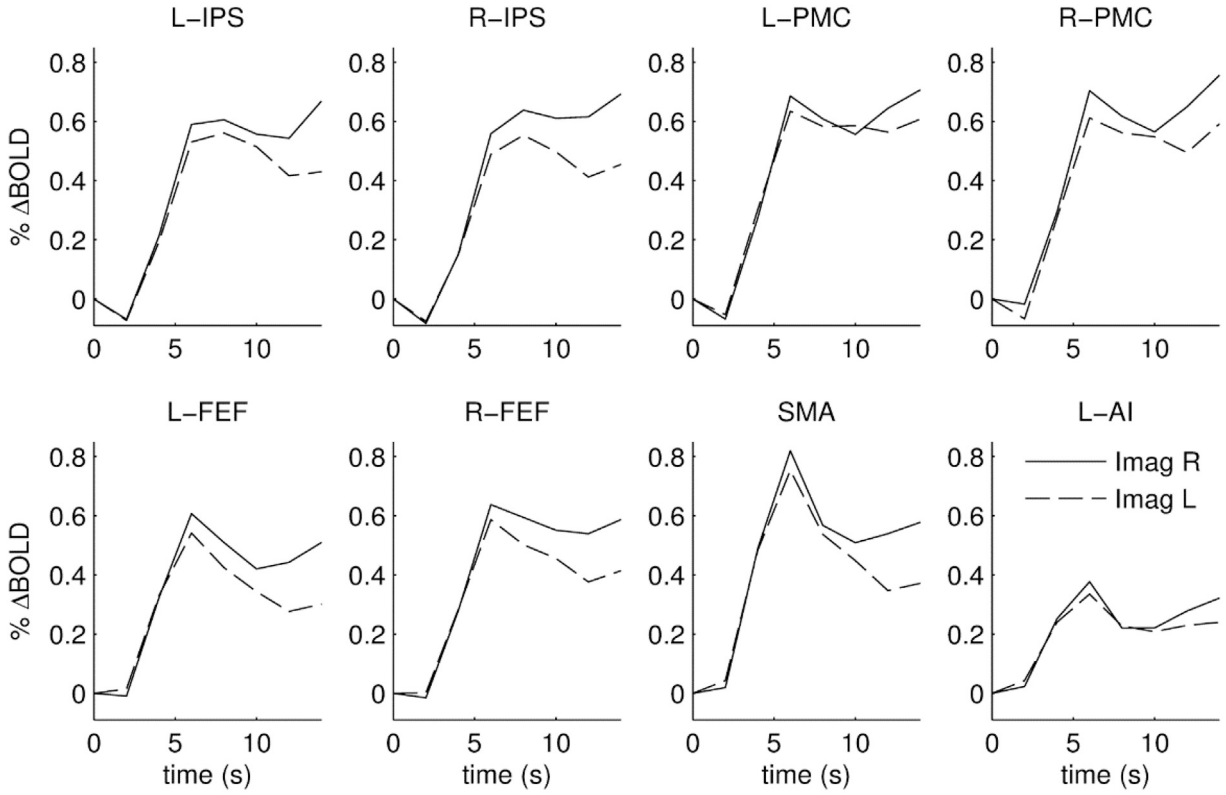

Fig. 10. Average BOLD response for participants in the experimental group during both left (dashed line) and right (solid line) imagery, and both imagery localizer runs, in the clusters seen in Fig. 9. Abbreviations same as in Fig. 9. L: left, R: right.

up- or downregulated in a task-dependent fashion via feedback modulations (Bullier, 2001; Roelfsema and de Lange, 2016). In this framework, the role of parietal cortex would be to provide that feedback to early visual cortex, and to keep the mental image active over an extended period, possibly in a joint effort with frontal regions. In line with this view, using dynamic causal modelling of fMRI data, Dijkstra et al. (2017a,b) found that stronger vividness gave stronger excitatory influence from parietal cortex to occipital cortex during visual imagery. Based on this, our finding that parietal cortex is more sensitive to focus and vividness of visual imagery than early visual cortex is somewhat unexpected. We believe that this observation would be worth further investigations in follow-up studies, ideally in a paradigm that would allow trial-wise ratings of both focus and vividness, to help us better understand the underlying dynamics.

Two regions, SMA and R-PMC, seemed largely unaffected by the vividness rating. SMA is reported to be recruited during imagery in different sensory modalities, and it has for instance been suggested that the region facilitates flexible engagement of sensorimotor processes that in turn enable auditory imagery (Lima et al., 2016). This functionality could be extended to visual imagery and thus would not rely strongly on visual vividness. The difference between the left and right PMC could be explained by the two network theory suggested by Sack et al. (2008), where only the later network includes the left PMC.

Amedi et al. (2005) examined regions showing a negative BOLD response during visual imagery. Specifically, they correlated the participants' VVIQ score with the amplitude of the BOLD signal in areas deactivated or activated during the task. They found a negative correlation in auditory cortex and a positive correlation in visual areas, somatosensory areas and inferior prefrontal cortex. Likewise, Dijkstra et al., (2017a) obtained a parametric modulation of the BOLD response as a

Table 1
Descriptions of the kind of images the participant imagined during feedback runs. Two experimental participants did not provide a specific description of image types for one of their sessions and one control participant for both of the sessions. E: experimental group, C: control group.

Participant (E: experimental, C: control)	Strategy E: ROI_O session, C: Session 1	Strategy E: ROI_P session, C: Session 2
E1	Checkerboard, familiar things.	People on black and white background.
E2	Family members.	Family members.
E3	Mother's face, university, cars, random people, vegetables.	Familiar people, fruits and vegetables.
E4	Weird and chaotic images.	Checkerboard.
E5	*No description.*	Mother, girlfriend, eating breakfast.
E6	*No description.*	Familiar people.
E7	Checkerboard, rotating wheel, rainbow.	Flickering, rotating and exploding checkerboard and dancing people.
E8	Checkerboard, people.	Actions.
E9	Checkerboard.	Checkerboard.
E10	Familiar faces, shark attack.	Checkerboard.
E11	Checkerboard.	Checkerboard.
E12	Checkerboard.	Checkerboard.
E13	Checkerboard, friends' faces, snow, fireworks, the sea, children playing.	Checkerboard.
E14	Checkerboard.	Looking out a window, street with cars, pets.
C1	Interesting images.	Food.
C2	Checkerboard, fruit.	Checkerboard.
C3	Walking home, taking the bus, getting on a plane, cooking.	Checkerboard, everyday actions.
C4	Checkerboard.	Checkerboard.
C5	Checkerboard.	Checkerboard.
C6	Trees, familiar objects, familiar actions.	Familiar actions.
C7	*No description.*	*No description.*

function of vividness in early visual cortex, the precunues, medial frontal cortex, and right parietal cortex. Together, these results clearly demonstrate that vividness contributes to the variability of the BOLD response in a number of areas recruited during visual imagery. The results of the current study moreover suggest that a subjective rating of individual runs might be preferable to a more general measure such as the one available from the VVIQ (Dijkstra et al., 2017a). By not capturing the variation in focus and vividness during the experiment, or between experiments, one will not be able to explain the corresponding variance in the neuroimaging data. Future studies might therefore profit from such individual ratings to examine how different regions are affected by mental focus and imagery vividness (Amedi et al., 2005; Cui et al., 2007; Lee et al., 2012; Motoyama and Hishitani, 2016; Scharnowski et al., 2012). By studying different regions' susceptibility to neurofeedback learning and how they are affected by mental focus and imagery vividness we can gain insight in the complex network that produces and maintains our inner mental images. One suggestion could be to target content-dependent regions (Schwarzlose et al., 2008) (e.g. the fusiform face area (Ishai et al., 2002; Kanwisher et al., 1997), the extrastriate body area (Downing et al., 2001), the parahippocampal place area (Epstein and Kanwisher, 1998; O'Craven and Kanwisher, 2000) and the lateral occipital area (Grill-Spector et al., 2001) to study how learned self-regulation and a strong vividness of content-specific features affect the activation in the target and other visual-network regions as well as the performance in behavioral tasks (Cui et al., 2007; Tartaglia et al., 2009). In a clinical setting, targeting content-dependent regions could potentially make it possible to apply neurofeedback for treating category-specific agnosias, such as prosopagnosia.

Table 2
Number of voxels, number of connected clusters and maximum t value for ROI_O (from the stimulus localizer) and ROI_P (from the imagery localizer). For participants in the control group, values from the control ROI (bilateral ventral striatum) in Session 1 and Session 2 are provided. E: experimental group, C: control group.

Participant (E: experimental, C: control)	Nr voxels E: ROI_O, C: V.Str. Session 1	Nr clusters E: ROI_O, C: V.Str. Session 1	t_{max} ROI_O	Nr voxels E: ROI_P, C: V.Str. Session 2	Nr clusters E: ROI_P, C: V.Str. Session 2	t_{max} ROI_P
E1	50	2	12.7	19	4	4.9
E2	47	3	9.9	8	1	2.9
E3	41	3	12.1	20	2	6.7
E4	48	2	11.5	8	2	2.3
E5	45	2	15.1	19	1	2.8
E6	42	2	14.3	14	3	2.3
E7	42	6	18.7	16	4	3.5
E8	49	3	10.2	10	2	2.7
E9	48	2	13.9	11	2	2.0
E10	48	1	20.8	20	2	5.9
E11	41	2	13.3	13	2	4.8
E12	44	3	7.3	10	1	4.3
E13	44	1	16.0	20	2	2.8
E14	24	2	5.8	19	2	4.6
C1	41	2	-	53	2	-
C2	43	2	-	75	2	-
C3	77	2	-	67	2	-
C4	72	2	-	65	2	-
C5	69	2	-	67	2	-
C6	40	2	-	48	2	-
C7	40	2	-	49	2	-

Table 3
The Spearman rank correlation coefficients (ρ) between the BOLD signal at 6 s in the ROIs and the subjective rating of focus and vividness for each imagery localizer and feedback run. The p-values, for testing the hypothesis of no correlation, are shown in brackets. * denotes significance at $\alpha = 0.05$.

	Focus	Vividness
ROI_O	$\rho = -0.08$ ($p = 0.58$)	$\rho = -0.09$ ($p = 0.52$)
ROI_P	$\rho = -0.34$ ($p = 0.01$) *	$\rho = -0.45$ ($p < 0.01$) *

Table 4
MNI coordinates (of peak), number of voxels and peak t-values for the significant clusters (L: left, R: right) from the group analysis of imagery localizer 1 for the contrast "imagery right + imagery left". Voxel size is 3 mm isotropic since computations are based on spatially normalized data (abbreviations same as in Fig. 9).

Area	X	y	z	Size	t_{max}
SMA	−3	6	54	64	7.03
L-AI	−36	18	0	96	10.93
L-FEF	−27	−3	51	133	8.24
R-FEF	30	−3	54	74	9.39
L-IPS	−36	−42	45	318	9.32
R–IPS	36	−42	51	115	7.38
L-PMC	−51	9	39	45	8.98
R-PMC	54	6	39	35	6.84

4.2. *Visual imagery in the medial superior parietal lobe*

The MSPL is known to host a variety of different functionalities requiring spatial processing. For example, seven maps of the contralateral visual field have been described along the intraparietal sulcus (IPS0-5) and the superior parietal lobule (SPL1) (Silson et al., 2016; Silver and Kastner, 2009; Wandell et al., 2007). Moreover, MSPL is involved in spatial attention (Andersson et al., 2012; Han et al., 2004; Kastner et al., 1999), the planning and execution of prehension movements (Ariani

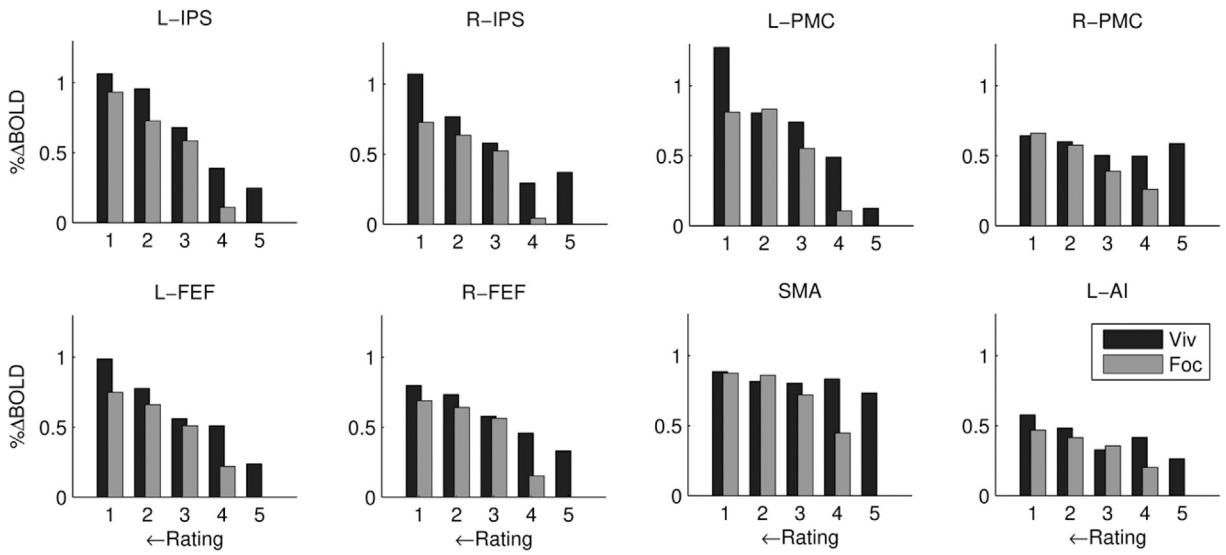

Fig. 11. The mean response at the 6s peak inside the clusters seen in Fig. 9 for the experimental group in all imagery localizer and feedback runs, ordered according to individual ratings of focus and vividness (abbreviations same as in Fig. 9. L: left, R: right).

Table 5
The Spearman rank correlation coefficients (ρ) between the BOLD signal at 6 s in the clusters seen in Fig. 9 and the subjective rating of focus and vividness for each imagery localizer and feedback run. The p-values, for testing the hypothesis of no correlation, are shown in brackets. * denotes significance at $\alpha = 0.01$.

	Focus	Vividness
L-IPS	$\rho = -0.39$ ($p < 0.001$) *	$\rho = -0.47$ ($p < 0.001$) *
R–IPS	$\rho = -0.30$ ($p = 0.001$) *	$\rho = -0.44$ ($p < 0.001$) *
L-PMC	$\rho = -0.30$ ($p = 0.002$) *	$\rho = -0.30$ ($p = 0.002$) *
R-PMC	$\rho = -0.28$ ($p = 0.003$) *	$\rho = -0.13$ ($p = 0.174$)
L-FEF	$\rho = -0.31$ ($p < 0.001$) *	$\rho = -0.38$ ($p < 0.001$) *
R-FEF	$\rho = -0.25$ ($p = 0.008$) *	$\rho = -0.35$ ($p < 0.001$) *
SMA	$\rho = -0.22$ ($p = 0.020$)	$\rho = 0.00$ ($p = 0.961$)
L-AI	$\rho = -0.28$ ($p = 0.003$) *	$\rho = -0.27$ ($p = 0.004$) *

et al., 2015; Turella et al., 2016), sensorimotor integration (Wolpert et al., 1998) and working memory (Koenigs et al., 2009; Sheremata et al., 2010). The topographic processing makes MSPL an interesting candidate target region for neurofeedback if the goal is to focus on a particular location of the visual field.

Our participants were instructed to perform visual imagery within the upper right quadrant. It is evident that this task has a clear spatial component and is attentionally demanding (Corbetta and Shulman, 2002). An idea for future research would be to replicate the present study using imagery in the foveal region to see if the MSPL response changes as the mental image is projected in a place demanding less effort on spatial attention. This can for instance be relevant when the goal is visual rehabilitation of a foveal region of the visual field via restorative neurofeedback training. A more dedicated localizer could be applied to pinpoint one of the functional maps located in MSPL.

Moreover, by learning more about the medial parietal areas' involvement in covert mental processes such as imagery could potentially inform us on their roles in the default mode network as proposed by a growing number of studies (Andrews-Hanna et al., 2010; Axelrod et al., 2017; Baldassano et al., 2016; Bzdok et al., 2015).

4.3. The visual imagery network

The group analysis identified eight regions recruited during both left and right visual imagery, confirming previous findings. PMC has previously been shown to be recruited during visual imagery (Richter et al., 2000; Sack et al., 2008). SMA has been shown to be recruited during visual (Richter et al., 2000), motor (Gerardin et al., 2000), auditory (Halpern and Zatorre, 1999; Lima et al., 2016) and even olfactory imagery (Djordjevic et al., 2005).

The FEF is believed to be involved in a number of tasks, including attentional selection, suppression of eye-movements and maintaining a mental image (Gilbert and Li, 2013; Zvyagintsev et al., 2013). This is supported by the fact that the response, especially in the left FEF, is largely maintained over the block.

The IPS is known to be involved in spatial attention processing (Hopfinger et al., 2000; Ishai et al., 2002) and has been suggested to provide top-down feedback to early visual cortex during visual imagery (Dijkstra et al., 2017b).

Using fuzzy clustering and Granger causality mapping (GCM), Sack et al. (2008) distinguished two frontoparietal networks processing visual imagery, one recruited slightly earlier than the other. Both networks showed an information flow from PMC to IPS, but while the network recruited earlier was bilateral in nature, the network recruited slightly later was more lateralized towards the left hemisphere. This could possibly be related to why we see a difference in the effect of vividness between R-PMC and L-PMC (Table 5).

The L-AI has previously been shown to be recruited during similar tasks. A positron emission tomography (PET) study (Ghaem et al., 1997) found higher activation in L-AI during mental navigation compared to mental visualization of static landmarks. In another PET study (Mellet et al., 2000) on visual imagery that revealed recruitment of L-AI, the authors argued that the activity might be related to verbal rehearsal of the task. Bilateral AI was also found in an fMRI study comparing activation during visual imagery and visual perception (Ganis et al., 2004).

4.4. The time course of visual imagery

As expected, the stimulus localizer generated a much stronger response than the imagery localizer (Table 2). More importantly, Fig. 3 shows that the signal changes induced during visual imagery are comparable in the two ROIs.

The time-course of the BOLD responses in both the imagery localizers and feedback runs and in all regions (including the regions detected by the "right + left" contrast) peaked at around 6 s, which is in agreement with previous studies (Amedi et al., 2005; Klein et al., 2000). However, it should be noted that our study did not aim to examine detailed differences in timing, which would have required another type of paradigm. When comparing the post-peak signal in ROI_O and ROI_P, the latter

showed a more sustained response. This could possibly be seen in the light of the parietal area being a multi-functional hub involved in many aspects of mental imagery, for example spatial attention and memory integration. Further, it seems reasonable that one could activate the parietal regions by engaging some levels of the top-down processing chain needed to bring out and maintain a mental image, without necessarily being able to reach the end of the chain in the low level occipital visual regions (see also section 4.4).

5. Conclusion

Our findings demonstrate that both early visual cortex and MSPL are susceptible to auditory real-time neurofeedback. We observed a more sustained signal when feedback was provided from parietal in comparison to occipital cortex. Moreover, we found that the parietal ROI was more affected by participants' self-rated focus and vividness during imagery. These results suggest that MSPL might be a suitable region to provide real-time neurofeedback in patients with visual field defects, either when the cortical damage is located within MSPL or when the BOLD signal in a damaged primary visual cortex is too impaired to provide a useable neurofeedback signal. Moreover, this study shows that different nodes in the network recruited during visual imagery respond differently to neurofeedback, and thus that future studies could use it as a tool for separating different aspects of visual imagery. The study also shows that the influence of subjective vividness and focus are more complex than can be measured with a static VVIQ score.

Declarations of interest

None.

Acknowledgments

This research was supported by the European Research Council [grant number 339939].

References

Albers, A.M., Kok, P., Toni, I., Dijkerman, H.C., de Lange, F.P., 2013. Shared representations for working memory and mental imagery in early visual cortex. Curr. Biol. 23, 1427–1431. https://doi.org/10.1016/j.cub.2013.05.065.

Amedi, A., Malach, R., Pascual-Leone, A., 2005. Negative BOLD differentiates visual imagery and perception. Neuron 48, 859–872. https://doi.org/10.1016/j.neuron.2005.10.032.

Andersson, P., Pluim, J.P.W., Siero, J.C.W., Klein, S., Viergever, M.A., Ramsey, N.F., 2011. Real-time decoding of brain responses to visuospatial attention using 7T fMRI. PLoS One 6, e27638. https://doi.org/10.1371/journal.pone.0027638.

Andersson, P., Ramsey, N.F., Raemaekers, M., Viergever, M.A., Pluim, J.P.W., 2012. Real-time decoding of the direction of covert visuospatial attention. J. Neural Eng. 9, 045004.

Andrews-Hanna, J.R., Reidler, J.S., Sepulcre, J., Poulin, R., Buckner, R.L., 2010. Functional-anatomic fractionation of the brain's default network. Neuron 65, 550–562. https://doi.org/10.1016/j.neuron.2010.02.005.

Ariani, G., Wurm, M.F., Lingnau, A., 2015. Decoding internally and externally driven movement plans. J. Neurosci. 35, 14160–14171. https://doi.org/10.1523/JNEUROSCI.0596-15.2015.

Ashburner, J., 2007. A fast diffeomorphic image registration algorithm. Neuroimage 38, 95–113. https://doi.org/10.1016/j.neuroimage.2007.07.007.

Axelrod, V., Rees, G., Bar, M., 2017. The default network and the combination of cognitive processes that mediate self-generated thought. Nat. Hum. Behav. 1, 896–910. https://doi.org/10.1038/s41562-017-0244-9.

Baldassano, C., Esteva, A., Fei-Fei, L., Beck, D.M., 2016. Two Distinct Scene-Processing Networks Connecting Vision and Memory. eNeuro 3, ENEURO.0178-16.2016. https://doi.org/10.1523/ENEURO.0178-16.2016.

Brainard, D., 1997. The psychophysics toolbox. Spatial Vis. 433–436. https://doi.org/10.1163/156856897x00357.

Brodtmann, A., Puce, A., Darby, D., Donnan, G., 2015. Extrastriate visual cortex reorganizes despite sequential bilateral occipital stroke: implications for vision recovery. Front. Hum. Neurosci. 9. https://doi.org/10.3389/fnhum.2015.00224.

Bullier, J., 2001. Integrated model of visual processing. Brain res. Rev., the brain in health and disease - from molecules to man. In: Swiss National Foundation Symposium NRP, vol 38, pp. 96–107, 36. https://doi.org/10.1016/S0165-0173(01)00085-6.

Bzdok, D., Heeger, A., Langner, R., Laird, A.R., Fox, P.T., Palomero-Gallagher, N., Vogt, B.A., Zilles, K., Eickhoff, S.B., 2015. Subspecialization in the human posterior medial cortex. Neuroimage 106, 55–71. https://doi.org/10.1016/j.neuroimage.2014.11.009.

Corbetta, M., Shulman, G.L., 2002. Control of goal-directed and stimulus-driven attention in the brain. Nat. Rev. Neurosci. 3, 201–215. https://doi.org/10.1038/nrn755.

Cox, R.W., Jesmanowicz, A., Hyde, J.S., 1995. Real-time functional magnetic resonance imaging. Magn. Reson. Med. 33, 230–236.

Cui, X., Jeter, C.B., Yang, D., Montague, P.R., Eagleman, D.M., 2007. Vividness of mental imagery: individual variability can be measured objectively. Vision Res 47, 474–478. https://doi.org/10.1016/j.visres.2006.11.013.

de Borst, A.W., Sack, A.T., Jansma, B.M., Esposito, F., de Martino, F., Valente, G., Roebroeck, A., di Salle, F., Goebel, R., Formisano, E., 2012. Integration of "what" and "where" in frontal cortex during visual imagery of scenes. Neuroimage 60, 47–58. https://doi.org/10.1016/j.neuroimage.2011.12.005.

de Gelder, B., Tamietto, M., Pegna, A.J., Van den Stock, J., 2015. Visual imagery influences brain responses to visual stimulation in bilateral cortical blindness. Cortex 72, 15–26. https://doi.org/10.1016/j.cortex.2014.11.009.

de Haan, B., Rorden, C., Karnath, H.-O., 2013. Abnormal perilesional BOLD signal is not correlated with stroke patients' behavior. Front. Hum. Neurosci. 7. https://doi.org/10.3389/fnhum.2013.00669.

Dentico, D., Cheung, B.L., Chang, J.-Y., Guokas, J., Boly, M., Tononi, G., Van Veen, B., 2014. Reversal of cortical information flow during visual imagery as compared to visual perception. Neuroimage 100, 237–243. https://doi.org/10.1016/j.neuroimage.2014.05.081.

Dijkstra, N., Bosch, S., van Gerven, M.A.J., 2017a. Vividness of visual imagery depends on the neural overlap with perception in visual areas. J. Neurosci. 3022–16. https://doi.org/10.1523/JNEUROSCI.3022-16.2016.

Dijkstra, N., Zeidman, P., Ondobaka, S., Gerven, M. a. J., Friston, K., 2017b. Distinct top-down and bottom-up brain connectivity during visual perception and imagery. Sci. Rep. 7, 5677. https://doi.org/10.1038/s41598-017-05888-8.

Djordjevic, J., Zatorre, R.J., Petrides, M., Boyle, J.A., Jones-Gotman, M., 2005. Functional neuroimaging of odor imagery. Neuroimage 24, 791–801. https://doi.org/10.1016/j.neuroimage.2004.09.035.

Downing, P.E., Jiang, Y., Shuman, M., Kanwisher, N., 2001. A cortical area selective for visual processing of the human body. Science 293, 2470–2473. https://doi.org/10.1126/science.1063414.

Dundon, N.M., Bertini, C., Làdavas, E., Sabel, B.A., Gall, C., 2015. Visual rehabilitation: visual scanning, multisensory stimulation and vision restoration trainings. Front. Behav. Neurosci. 9. https://doi.org/10.3389/fnbeh.2015.00192.

Emmerling, T.C., Zimmermann, J., Sorger, B., Frost, M.A., Goebel, R., 2016. Decoding the direction of imagined visual motion using 7T ultra-high field fMRI. Neuroimage 125, 61–73. https://doi.org/10.1016/j.neuroimage.2015.10.022.

Epstein, R., Kanwisher, N., 1998. A cortical representation of the local visual environment. Nature 392, 598–601. https://doi.org/10.1038/33402.

Filimon, F., Nelson, J.D., Hagler, D.J., Sereno, M.I., 2007. Human cortical representations for reaching: mirror neurons for execution, observation, and imagery. Neuroimage 37, 1315–1328. https://doi.org/10.1016/j.neuroimage.2007.06.008.

Ganis, G., Thompson, W.L., Kosslyn, S.M., 2004. Brain areas underlying visual mental imagery and visual perception: an fMRI study. Cogn. Brain Res. 20, 226–241. https://doi.org/10.1016/j.cogbrainres.2004.02.012.

Gerardin, E., Sirigu, A., Lehéricy, S., Poline, J.-B., Gaymard, B., Marsault, C., Agid, Y., Bihan, D.L., 2000. Partially overlapping neural networks for real and imagined hand movements. Cerebr. Cortex 10, 1093–1104. https://doi.org/10.1093/cercor/10.11.1093.

Ghaem, O., Mellet, E., Crivello, F., Tzourio, N., Mazoyer, B., Berthoz, A., Denis, M., 1997. Mental navigation along memorized routes activates the hippocampus, precuneus, and insula. Neuroreport 8, 739–744.

Gilbert, C.D., Li, W., 2013. Top-down influences on visual processing. Nat. Rev. Neurosci. 14, 350–363. https://doi.org/10.1038/nrn3476.

Gourtzelidis, P., Tzagarakis, C., Lewis, S.M., Crowe, D.A., Auerbach, E., Jerde, T.A., Uğurbil, K., Georgopoulos, A.P., 2005. Mental maze solving: directional fMRI tuning and population coding in the superior parietal lobule. Exp. Brain Res. 165, 273–282. https://doi.org/10.1007/s00221-005-2298-6.

Grill-Spector, K., Kourtzi, Z., Kanwisher, N., 2001. The lateral occipital complex and its role in object recognition. Vision Res 41, 1409–1422. https://doi.org/10.1016/S0042-6989(01)00073-6.

Halpern, A.R., Zatorre, R.J., 1999. When that tune runs through your head: a PET investigation of auditory imagery for familiar melodies. Cerebr. Cortex 9, 697–704. https://doi.org/10.1093/cercor/9.7.697.

Hamamé, C.M., Vidal, J.R., Ossandón, T., Jerbi, K., Dalal, S.S., Minotti, L., Bertrand, O., Kahane, P., Lachaux, J.-P., 2012. Reading the mind's eye: online detection of visuo-spatial working memory and visual imagery in the inferior temporal lobe. Neuroimage 59, 872–879. https://doi.org/10.1016/j.neuroimage.2011.07.087.

Han, S., Jiang, Y., Gu, H., Rao, H., Mao, L., Cui, Y., Zhai, R., 2004. The role of human parietal cortex in attention networks. Brain 127, 650–659. https://doi.org/10.1093/brain/awh071.

Hopfinger, J.B., Buonocore, M.H., Mangun, G.R., 2000. The neural mechanisms of top-down attentional control. Nat. Neurosci. 3, 284–291. https://doi.org/10.1038/72999.

Hübener, M., Bonhoeffer, T., 2014. Neuronal plasticity: beyond the critical period. Cell 159, 727–737. https://doi.org/10.1016/j.cell.2014.10.035.

Ishai, A., Haxby, J.V., Ungerleider, L.G., 2002. Visual imagery of famous faces: effects of memory and attention revealed by fMRI. Neuroimage 17, 1729–1741. https://doi.org/10.1006/nimg.2002.1330.

Kanwisher, N., McDermott, J., Chun, M.M., 1997. The fusiform face area: a module in human extrastriate cortex specialized for face perception. J. Neurosci. 17, 4302–4311.

Kastner, S., Pinsk, M.A., De Weerd, P., Desimone, R., Ungerleider, L.G., 1999. Increased activity in human visual cortex during directed attention in the absence of visual stimulation. Neuron 22, 751–761. https://doi.org/10.1016/S0896-6273(00)80734-5.

Klein, I., Dubois, J., Mangin, J.-F., Kherif, F., Flandin, G., Poline, J.-B., Denis, M., Kosslyn, S.M., Le Bihan, D., 2004. Retinotopic organization of visual mental images as revealed by functional magnetic resonance imaging. Cogn. Brain Res. 22, 26–31. https://doi.org/10.1016/j.cogbrainres.2004.07.006.

Klein, I., Paradis, A.-L., Poline, J.-B., Kosslyn, S.M., Le Bihan, D., 2000. Transient activity in the human calcarine cortex during visual-mental imagery: an event-related fMRI study. J. Cogn. Neurosci. 12, 15–23. https://doi.org/10.1162/089892900564037.

Koenigs, M., Barbey, A.K., Postle, B.R., Grafman, J., 2009. Superior parietal cortex is critical for the manipulation of information in working memory. J. Neurosci. 29, 14980–14986. https://doi.org/10.1523/JNEUROSCI.3706-09.2009.

Kosslyn, S.M., Ganis, G., Thompson, W.L., 2001. Neural foundations of imagery. Nat. Rev. Neurosci. 2, 635–642. https://doi.org/10.1038/35090055.

Kosslyn, S.M., Thompson, W.L., 2003. When is early visual cortex activated during visual mental imagery? Psychol. Bull. 129, 723–746. https://doi.org/10.1037/0033-2909.129.5.723.

Lee, S.-H., Kravitz, D.J., Baker, C.I., 2012. Disentangling visual imagery and perception of real-world objects. Neuroimage 59, 4064–4073. https://doi.org/10.1016/j.neuroimage.2011.10.055.

Lima, C.F., Krishnan, S., Scott, S.K., 2016. Roles of supplementary motor areas in auditory processing and auditory imagery. Trends Neurosci. 39, 527–542. https://doi.org/10.1016/j.tins.2016.06.003.

Marks, D.F., 1973. Visual imagery differences in the recall of pictures. Br. J. Psychol. 64, 17–24. https://doi.org/10.1111/j.2044-8295.1973.tb01322.x.

Matteo, B.M., Viganò, B., Cerri, C.G., Perin, C., 2016. Visual field restorative rehabilitation after brain injury. J. Vis. 16, 11. https://doi.org/10.1167/16.9.11.

Mechelli, A., Price, C.J., Friston, K.J., Ishai, A., 2004. Where bottom-up meets top-down: neuronal interactions during perception and imagery. Cerebr. Cortex 14, 1256–1265. https://doi.org/10.1093/cercor/bhh087.

Mellet, E., Tzourio-Mazoyer, N., Bricogne, S., Mazoyer, B., Kosslyn, S.M., Denis, M., 2000. Functional anatomy of high-resolution visual mental imagery. J. Cogn. Neurosci. 12, 98–109. https://doi.org/10.1162/08989290051137620.

Motoyama, H., Hishitani, S., 2016. The brain mechanism that reduces the vividness of negative imagery. Conscious. Cognit. 39, 59–69. https://doi.org/10.1016/j.concog.2015.11.006.

O'Craven, K.M., Kanwisher, N., 2000. Mental imagery of faces and places activates corresponding stiimulus-specific brain regions. J. Cogn. Neurosci. 12, 1013–1023. https://doi.org/10.1162/08989290051137549.

Papageorgiou, T.D., Papanikolaou, A., Smirnakis, S., 2014. A systematic approach to visual system rehabilitation - population receptive field analysis and real-time functional magnetic resonance imaging neurofeedback methods. In: Advanced Brain Neuroimaging Topics in Health and Disease - Methods and Applications. InTech, pp. 371–402.

Pearson, J., Naselaris, T., Holmes, E.A., Kosslyn, S.M., 2015. Mental imagery: functional mechanisms and clinical applications. Trends Cognit. Sci. 19, 590–602. https://doi.org/10.1016/j.tics.2015.08.003.

Pflugshaupt, T., Nösberger, M., Gutbrod, K., Weber, K.P., Linnebank, M., Brugger, P., 2016. Bottom-up visual integration in the medial parietal lobe. Cerebr. Cortex 26, 943–949. https://doi.org/10.1093/cercor/bhu256.

Pleger, B., Foerster, A.-F., Widdig, W., Henschel, M., Nicolas, V., Jansen, A., Frank, A., Knecht, S., Schwenkreis, P., Tegenthoff, M., 2003. Functional magnetic resonance imaging mirrors recovery of visual perception after repetitive tachistoscopic stimulation in patients with partial cortical blindness. Neurosci. Lett. 335, 192–196. https://doi.org/10.1016/S0304-3940(02)01153-9.

Richter, W., Somorjai, R., Summers, R., Jarmasz, M., Menon, R.S., Gati, J.S., Georgopoulos, A.P., Tegeler, C., Ugurbil, K., Kim, S.-G., 2000. Motor area activity during mental rotation studied by time-resolved single-trial fMRI. J. Cogn. Neurosci. 12, 310–320. https://doi.org/10.1162/089892900562129.

Robineau, F., Saj, A., Neveu, R., Ville, D.V.D., Scharnowski, F., Vuilleumier, P., 2017. Using real-time fMRI neurofeedback to restore right occipital cortex activity in patients with left visuo-spatial neglect: proof-of-principle and preliminary results. Neuropsychol. Rehabil. 1–22. https://doi.org/10.1080/09602011.2017.1301262.

Roelfsema, P.R., de Lange, F.P., 2016. Early visual cortex as a multiscale cognitive blackboard. Annu. Rev. Vis. Sci. 2, 131–151. https://doi.org/10.1146/annurev-vision-111815-114443.

Sabel, B.A., Henrich-Noack, P., Fedorov, A., Gall, C., 2011. Chapter 13 - vision restoration after brain and retina damage: the "residual vision activation theory. In: Andrea Green, C.E.C., Kalaska, John F., Franco, Lepore (Eds.), Progress in Brain Research, Enhancing Performance for Action and PerceptionMultisensory Integration, Neuroplasticity and Neuroprosthetics, Part II. Elsevier, pp. 199–262.

Sack, A.T., Jacobs, C., Martino, F.D., Staeren, N., Goebel, R., Formisano, E., 2008. Dynamic premotor-to-parietal interactions during spatial imagery. J. Neurosci. 28, 8417–8429. https://doi.org/10.1523/JNEUROSCI.2656-08.2008.

Scharnowski, F., Hutton, C., Josephs, O., Weiskopf, N., Rees, G., 2012. Improving visual perception through neurofeedback. J. Neurosci. 32, 17830–17841. https://doi.org/10.1523/JNEUROSCI.6334-11.2012.

Scharnowski, F., Rosa, M.J., Golestani, N., Hutton, C., Josephs, O., Weiskopf, N., Rees, G., 2014. Connectivity changes underlying neurofeedback training of visual cortex activity. PLoS One 9, e91090. https://doi.org/10.1371/journal.pone.0091090.

Schwarzbach, J., 2011. A simple framework (ASF) for behavioral and neuroimaging experiments based on the psychophysics toolbox for MATLAB. Behav. Res. Methods 43, 1194–1201. https://doi.org/10.3758/s13428-011-0106-8.

Schwarzlose, R.F., Swisher, J.D., Dang, S., Kanwisher, N., 2008. The distribution of category and location information across object-selective regions in human visual cortex. Proc. Natl. Acad. Sci. Unit. States Am. 105, 4447–4452. https://doi.org/10.1073/pnas.0800431105.

Sheremata, S.L., Bettencourt, K.C., Somers, D.C., 2010. Hemispheric asymmetry in visuotopic posterior parietal cortex emerges with visual short-term memory load. J. Neurosci. 30, 12581–12588. https://doi.org/10.1523/JNEUROSCI.2689-10.2010.

Silson, E.H., Steel, A.D., Baker, C.I., 2016. Scene-selectivity and retinotopy in medial parietal cortex. Front. Hum. Neurosci. 10. https://doi.org/10.3389/fnhum.2016.00412.

Silver, M.A., Kastner, S., 2009. Topographic maps in human frontal and parietal cortex. Trends Cognit. Sci. 13, 488–495. https://doi.org/10.1016/j.tics.2009.08.005.

Slotnick, S.D., Thompson, W.L., Kosslyn, S.M., 2005. Visual mental imagery induces retinotopically organized activation of early visual areas. Cerebr. Cortex 15, 1570–1583. https://doi.org/10.1093/cercor/bhi035.

Smania, N., Bazoli, F., Piva, D., Guidetti, G., 1997. Visuomotor imagery and rehabilitation of neglect. Arch. Phys. Med. Rehabil. 78, 430–436. https://doi.org/10.1016/S0003-9993(97)90237-9.

Stoeckel, L.E., Garrison, K.A., Ghosh, S.S., Wighton, P., Hanlon, C.A., Gilman, J.M., Greer, S., Turk-Browne, N.B., deBettencourt, M.T., Scheinost, D., Craddock, C., Thompson, T., Calderon, V., Bauer, C.C., George, M., Breiter, H.C., Whitfield-Gabrieli, S., Gabrieli, J.D., LaConte, S.M., Hirshberg, L., Brewer, J.A., Hampson, M., Van Der Kouwe, A., Mackey, S., Evins, A.E., 2014. Optimizing real time fMRI neurofeedback for therapeutic discovery and development. NeuroImage Clin 5, 245–255. https://doi.org/10.1016/j.nicl.2014.07.002.

Sulzer, J., Haller, S., Scharnowski, F., Weiskopf, N., Birbaumer, N., Blefari, M.L., Bruehl, A.B., Cohen, L.G., deCharms, R.C., Gassert, R., Goebel, R., Herwig, U., LaConte, S., Linden, D., Luft, A., Seifritz, E., Sitaram, R., 2013. Real-time fMRI neurofeedback: progress and challenges. Neuroimage 76, 386–399. https://doi.org/10.1016/j.neuroimage.2013.03.033.

Tartaglia, E.M., Bamert, L., Mast, F.W., Herzog, M.H., 2009. Human perceptual learning by mental imagery. Curr. Biol. 19, 2081–2085. https://doi.org/10.1016/j.cub.2009.10.060.

Trauzettel-Klosinski, S., 2011. Current methods of visual rehabilitation. Dtsch. Ärztebl. Int. 108, 871–878. https://doi.org/10.3238/arztebl.2011.0871.

Trojano, L., Grossi, D., Linden, D.E.J., Formisano, E., Goebel, R., Cirillo, S., Elefante, R., Di Salle, F., 2002. Coordinate and categorical judgements in spatial imagery. An fMRI study. Neuropsychologia 40, 1666–1674. https://doi.org/10.1016/S0028-3932(02)00021-0.

Turella, L., Tucciarelli, R., Oosterhof, N.N., Weisz, N., Rumiati, R., Lingnau, A., 2016. Beta band modulations underlie action representations for movement planning. Neuroimage 136, 197–207. https://doi.org/10.1016/j.neuroimage.2016.05.027.

Urbanski, M., Coubard, O.A., Bourlon, C., 2014. Visualizing the blind brain: brain imaging of visual field defects from early recovery to rehabilitation techniques. Front. Integr. Neurosci. 8, 74. https://doi.org/10.3389/fnint.2014.00074.

Wandell, B.A., Dumoulin, S.O., Brewer, A.A., 2007. Visual field maps in human cortex. Neuron 56, 366–383.

Whittingstall, K., Bernier, M., Houde, J.-C., Fortin, D., Descoteaux, M., 2014. Structural network underlying visuospatial imagery in humans. Cortex. The clin. Neuroanat. of the occipital lobes 56, 85–98. https://doi.org/10.1016/j.cortex.2013.02.004.

Wolpert, D.M., Goodbody, S.J., Husain, M., 1998. Maintaining internal representations: the role of the human superior parietal lobe. Nat. Neurosci. 1, 529–533. https://doi.org/10.1038/2245.

Zvyagintsev, M., Clemens, B., Chechko, N., Mathiak, K.A., Sack, A.T., Mathiak, K., 2013. Brain networks underlying mental imagery of auditory and visual information. Eur. J. Neurosci. 37, 1421–1434. https://doi.org/10.1111/ejn.12140.